Deterministic stochastic resonance in a piecewise linear chaotic map

Sitabhra Sinha[1] and Bikas K. Chakrabarti[2]

[1]*Machine Intelligence Unit, Indian Statistical Institute, Calcutta 700 035, India*
[2]*Saha Institute of Nuclear Physics, 1/AF Bidhan Nagar, Calcutta 700 064, India*

The phenomenon of stochastic resonance (SR) is observed in a completely deterministic setting—with thermal noise being replaced by one-dimensional chaos. The piecewise linear map investigated in the paper shows a transition from symmetry-broken to symmetric chaos on increasing a system parameter. In the latter state, the chaotic trajectory switches between the two formerly disjoint attractors, driven by the map's inherent dynamics. This chaotic switching rate is found to ''resonate'' with the frequency of an externally applied periodic perturbation (multiplicative or additive). By periodically modulating the parameter at a specific frequency ω, we observe the existence of resonance where the response of the system (in terms of the residence-time distribution) is maximum. This is a clear indication of SR-like behavior in a chaotic system. [S1063-651X(98)03112-7]

Stochastic resonance (SR) is a recently observed nonlinear phenomena in noisy systems, where the noise helps in amplifying a subthreshold signal (which would have been otherwise undetected) when the signal frequency is close to a critical value [1]. This occurs because of noise-induced hopping between multiple stable states of a system, locking on to an externally imposed periodic signal. The characteristic signature of SR is the nonmonotonic nature of the signal-to-noise ratio (SNR) as a function of the external noise intensity. A theoretical understanding of this phenomena in bistable systems, subject to both periodic and random forcing, has been obtained based on the rate equation approach [2]. As the output of a chaotic process is indistinguishable from that of a noisy system, the question of whether a similar process occurs in the former case has long been debated. In fact, the authors of Ref. [1] indicated that the Lorenz system of equations, a well-known paradigm of chaotic behavior, might be showing SR. Later studies [3,4], in both discrete- and continuous-time systems, seemed to support this view. However, it is difficult to guarantee that the response behavior is due to ''resonance'' and not due to ''forcing.'' In the latter case, the periodic perturbation is of so large an amplitude that the system is forced to follow the driving frequency of the periodic forcing. The ambiguity is partly because the SNR is a monotonically decreasing function of the forcing frequency, and cannot be used to distinguish between resonance and forcing.

The signature of SR can also be observed in the residence time distribution. In the presence of a periodic modulation, the distribution shows a number of peaks superposed on an exponential background. However, this is observed both in the case of resonance as well as forcing. The ambiguity is, therefore, present in theoretical [5] and experimental [6] studies of noise-free SR, where regular and chaotic phases take the role of the two stable states in conventional SR. Although the distribution of the lengths of the chaotic interval shows a multipeaked structure, this by itself is not sufficient to ensure that the enhanced response is not due to forcing. In the present work this problem is avoided by measuring the response of the system in terms of the peaks in the normalized distribution of residence times [7]. For SR, the strength of the peaks shows nonmonotonicity with the variation of both noise intensity and signal frequency.

Ippen, Lindner, and Ditto [8] have used a chaotic driving term to show SR-like behavior in the SNR of the system response. However, in this case the chaos is supplied from outside, and not inherent to the system. Indeed, this distinction between stochastic and chaotic driving is somewhat artificial as, e.g., random numbers for Monte Carlo simulations are generated using chaos. If SR is actually used for information processing by biological systems, then it is likely that organs producing chaotic behavior might enhance their survival capability through selective amplification of signals in a noisy background. In this case, the inherent chaos of the system itself could play the role of ''noise.'' In the model proposed in this paper, a simple one-dimensional map has been shown to use its inherent chaoticity to replicate SR-like phenomena. This suggests a deep relation between stochastic resonance, on the one hand, and crises in chaotic dynamics, on the other hand, mentioned in Ref. [9]. The present work also supports this view.

The simplest chaotic system to show SR-type behavior are one-dimensional maps with two critical points. The most commonly studied system of this kind is the cubic map [10] $x_{n+1} = ax_n^3 + (1-a)x_n$, where a is a tunable parameter. The map is found to consist of two attractors, the initial condition determining the attractor into which the system settles. Various properties of such 'bimodal' maps differ from those observed for the well-studied class of maps with a single critical point (e.g., the logistic map).

Recently, SR has been studied in one-dimensional (1D) maps with two well-defined states (but not necessarily stable) with switching between them aided by either additive or multiplicative external noise [11]. However, dynamical contact of two chaotic 1D maps can also induce rhythmic hopping between the two domains of the system [12]. The present work shows how the chaotic dynamics of a system can itself be used for resonant switching between two states, without introducing any external noise.
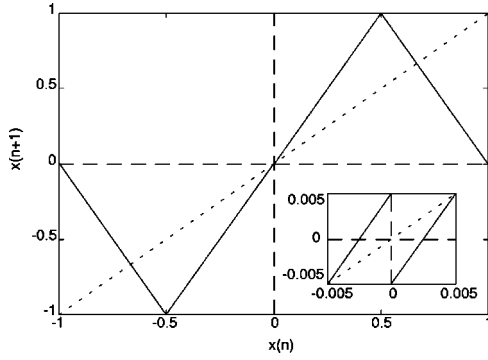
FIG. 1. The DAT map for $a_0 = 2.01$. Inset: a magnified view of the map in the interval $[-0.005, 0.005] \times [-0.005, 0.005]$.

The model chosen here is a piecewise linear bimodal map, henceforth referred to as the discontinuous antisymmetric tent (DAT) map, defined in the interval $[-1,1]$

$$x(n+1) = F(x_n)$$

$$= \begin{cases} 1 + a[0.5 - x(n)] & \text{if } x(n) \geq 0.5 \\ 1 - a[0.5 - x(n)] & \text{if } 0 < x(n) < 0.5 \\ -1 + a[0.5 + x(n)] & \text{if } -0.5 < x(n) < 0 \\ -1 - a[0.5 + x(n)] & \text{if } x(n) \leq -0.5. \end{cases} \quad (1)$$

The map has a discontinuity at $x = 0$. The behavior of the system was controlled by the parameter a ($0 < a < 4$). The onset of chaos occurs at $a = 1$. The chaos is symmetry broken, i.e., the trajectory is restricted to either of the two subintervals $R:(0,1]$ and $L:(0,-1]$, depending on initial condition. Symmetry is restored at $a = 2$. The Lyapunov exponent of the map is a simple monotonic function of the parameter a. The piecewise linear nature of the map makes its behavior simpler to study than, say, the cubic map described above. The map is shown in Fig. 1, the inset giving a detailed picture of the region around the discontinuity at $x = 0$. Figure 2 shows the evolution of the map's attractor with a increasing from 0 to 4.
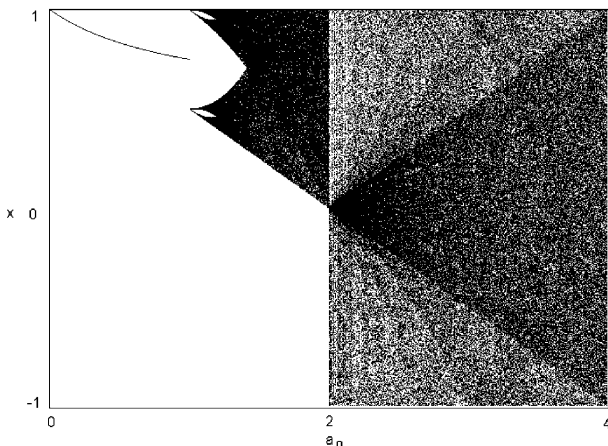

FIG. 2. Attractor of the DAT map vs a_0. The figure was obtained for $x_0 \in R$. For $x_0 \in L$ the corresponding image is obtained by reflecting about the x axis.
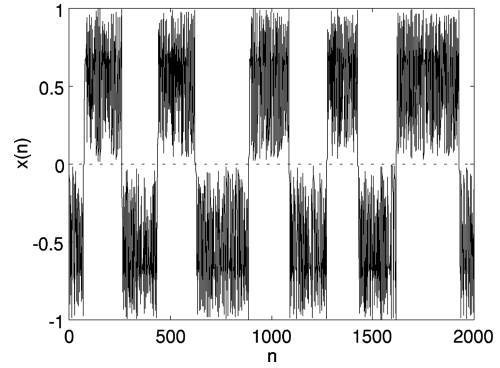

FIG. 3. The time evolution of the sinusoidally perturbed DAT map for $a_0 = 2.01$, $\omega = \frac{1}{400}$, and $\delta = 0.05$. The broken line is the boundary between L and R.

The map has a symmetrical pair of fixed points $x^*_{1,2} = \pm(1 + a/2)/(1 + a)$ which are stable for $0 < a < 1$ and unstable for $a > 1$. Another pair of unstable fixed points, $x^*_{3,4} = \pm(1 - a/2)/(1 - a)$ come into existence for $a > 2$. It is to be noted that as $a \to 2$ from above, $x^*_{3,4}$ both collide at $x = 0$ causing an interior crisis, which leads to symmetry breaking of the chaotic attractor.

To observe SR, the value of a was kept close to 2, and then modulated sinusoidally with amplitude δ and frequency ω, i.e.,

$$a_{n+1} = \begin{cases} a_0 + \delta \sin(2\pi \omega n) & \text{if } x \in R \\ a_0 - \delta \sin(2\pi \omega n) & \text{if } x \in L. \end{cases} \quad (2)$$

We refer to this henceforth as multiplicative or parametric perturbation, to distinguish it from additive perturbation (discussed later).

The system immediately offers an analogy to the classical bistable well scenario of SR. The sub intervals L and R correspond to the two wells between which the system hops to and fro, aided by the inherent noise (chaos) and the periodic signal. In each positive (negative) half-cycle of the periodic signal, a portion of the map defined over R (L) overlaps into the domain of the other portion defined over L (R). This is analogous to the successive raising and lowering of the wells in synchronization with the signal frequency, allowing the system to escape from one well to the other. The resultant intermittent switching of the trajectory between L and R is shown in Fig. 3. If the dynamics of the system due to the internal noise (chaos) has some inherent time scale (say n_k), as $1/\omega \to n_k$, the two time scales may lock onto each other. This resonance should be observable through an increase in the response characteristics of the map.

The response of the system is measured in terms of the normalized distribution of residence times, $N(n)$ [7]. This distribution shows a series of peaks centered at $n_j = (j - \frac{1}{2})n_0$, i.e., odd-integral multiples of the forcing period, $n_0 = 1/\omega$. The strength of the jth peak,

$$P_j = \int_{n_j - \alpha n_0}^{n_j + \alpha n_0} N(n) dn (0 < \alpha < 0.25), \quad (3)$$

is obtained at different values of ω, keeping a_0 fixed for $j = 1$, 2, and 3. To maximize sensitivity, α was taken to be

0.25. For $a_0 = 2.01$ and $\delta = 0.05$, the response of the system showed a nonmonotonic behavior as ω was varied, with P_1 peaking at $\omega_1 \sim \frac{1}{400}$, a value dependent upon a_0—a clear signature of a SR-type phenomenon. P_2 and P_3 also showed a nonmonotonic behavior, peaking roughly at odd-integral multiples of ω_1 [Fig. 4(a)]. For $a_0 < 2$, P_1 increases monotonically to 1 with decreasing ω, while, $P_j (j > 1)$ goes down to zero. So, ''true resonance,'' signified by the nonmonotonic profile of P_1, occurs only for $a_0 > 2$.

Similar observations of P_j were done also by varying a_0 keeping ω fixed. Figure 4(b) shows the results of simulations for $\omega = \frac{1}{400}$ and $\delta = 0.05$. Here also a nonmonotonicity was observed for P_1, P_2, and P_3. The broadness of the response curve and the magnitude of the peak strengths are a function of the perturbation magnitude, δ. The variation of P_1 with a_0 for different values of δ were also studied. As δ decreases, the response curve becomes more sharply peaked while the peak strength decreases.

Note that the parametric perturbation cannot be done without modulating the noise intensity. This seems to be the difference between this type of chaotic resonance and classical SR. As the local slope of the map, a, is varied periodically, the internal noise, whose intensity is a function of the Lyapunov exponent (and hence of a) also varies periodically. In contrast, for classical SR, the wells are raised or lowered periodically without affecting the external noise, which is independent of the geometry of the wells.

Analytical calculations were done to obtain the invariant probability density and the dominant time scale governing the residence-time distribution. This was done by proper partitioning of the domain of definition of the system and obtaining the eigenvalues of the corresponding transition matrix. From Fig. 2, it is clear that the system spends a longer time in the interval $[-\epsilon/2, \epsilon/2]$, where $\epsilon = a_0 - 2$. So a natural partitioning of the interval $[-1, 1]$ is into the four subintervals: C_1: $[-1, -\epsilon/2]$, C_2: $[-\epsilon/2, 0]$, C_3: $[0, \epsilon/2]$, and C_4: $[\epsilon/2, 1]$. This is an exactly Markov partition at integral values of ϵ, i.e., the partition boundaries $\{p_i\}$ transform into each other on application of the map dynamics ($f(p_j) \in \{p_i\}$). It is assumed that for $\epsilon \to 0$ the partitioning approximately retains its Markovian character, so that the process can be mapped onto a Markov process. Close to $\epsilon = 0$, the transition matrix corresponding to the above partitioning is

$$W = \begin{vmatrix} \dfrac{1-\epsilon/2-\epsilon^2/4}{1-\epsilon^2/4} & \dfrac{\epsilon}{4(1-\epsilon^2/4)} & \dfrac{\epsilon}{4(1-\epsilon^2/4)} & 0 \\[3mm] \dfrac{\epsilon}{2+\epsilon} & \dfrac{1}{2+\epsilon} & \dfrac{1}{2+\epsilon} & 0 \\[3mm] 0 & \dfrac{1}{2+\epsilon} & \dfrac{1}{2+\epsilon} & \dfrac{\epsilon}{2+\epsilon} \\[3mm] 0 & \dfrac{\epsilon}{4(1-\epsilon^2/4)} & \dfrac{\epsilon}{4(1-\epsilon^2/4)} & \dfrac{1-\epsilon/2-\epsilon^2/4}{1-\epsilon^2/4} \end{vmatrix}, \tag{4}$$

where $W_{ij} = P(C_i, C_j)$ is the probability of transition from C_i to C_j. The eigenvalues of the above matrix are $\lambda_1 = 1$, $\lambda_2 = (1 - \epsilon/2 - \epsilon^2/4)/(1 - \epsilon^2/4)$, $\lambda_3 = (1 - \epsilon)/(1 - \epsilon^2/4,)$ and $\lambda_4 = 0$. The largest eigenvalue 1 corresponds to the invariant
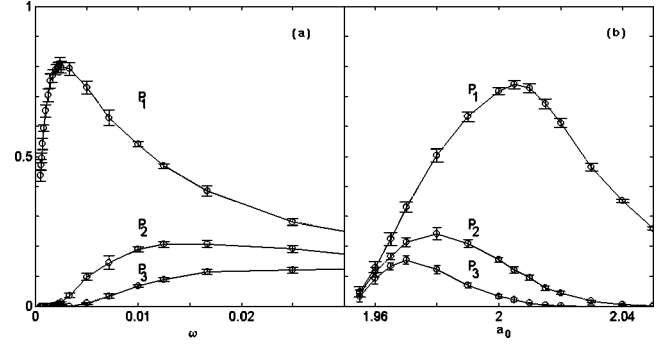

FIG. 4. (a) P_n ($n = 1, 2, 3$) vs ω for $a_0 = 2.01$ and $\delta = 0.05$, (b) P_n ($n = 1, 2, 3$) vs a_0 for $\omega = \frac{1}{400}$ and $\delta = 0.05$. The circles represent the average value of P_n for 18 different initial values of x, and the bars represent the standard deviation. The data points are joined by solid lines for the reader's convenience.

probability density over the four intervals. The next largest eigenvalue dominates any time-dependent phenomena. The relevant time scale (i.e., the mean residence time) is given by [3]

$$n_k = \frac{-1}{\ln\left(\dfrac{1-\epsilon/2-\epsilon^2/4}{1-\epsilon^2/4}\right)} \simeq \frac{-1}{\ln(1-\epsilon/2)}. \tag{5}$$

So, for $a_0 = 2.01$, $n_k \simeq 200$. This predicts that a peak in the response should be observed at a frequency $1/2n_k \simeq 1/400$, which agrees with the simulation results. For small ϵ, $\lambda_2 \simeq \exp(-\epsilon/2)$. Therefore, as $a_0 \to 2$ from above, the residence time diverges as

$$n_k \sim (a_0 - a_0^*)^{-1}, \quad a_0^* = 2. \tag{6}$$

The mean time spent by the trajectory in any one of the subintervals (L or R) can be calculated exactly for piecewise linear maps [13]. For $\epsilon > 0$, the intervals $\beta_1 = [0, \epsilon/2(2 + \epsilon)]$ and $\beta_2 = [1 - [\epsilon/2(2 + \epsilon)], 1]$ of R maps to L, so that the trajectory escapes from one subinterval to the other. Note the symmetrical placement of the two $R \to L$ ''escape regions'' about $x = 0.5$, because of the symmetry $F(1/2 - x) = F(1/2 + x)$ of the DAT map. So the total fraction of R escaping to L after one iteration is $l_1 = 2\epsilon/2(2 + \epsilon)$. Let us now consider the first preimage of β_1 and β_2, which escapes from R to L after two iterations. The total fraction of R belonging to this set is $l_2 = 4\epsilon/2(2 + \epsilon)^2$. Proceeding in this manner, we find from the geometry of the map that the total fraction of R which maps to L after n iterations, is

$$l_n = \frac{2^n \epsilon}{2(2 + \epsilon)^n}. \tag{7}$$

These are just the probabilities that the trajectory spends a period of n iterations in R before escaping to L ($\sum_{j=1}^{\infty} l_j = 1$). So the average lifetime of a trajectory in R is

$$\langle n \rangle = \sum_{j=1}^{\infty} (j-1)l_j = \frac{2}{\epsilon}. \tag{8}$$

For $a_0 = 2.01$, $\langle n \rangle = 200$, in good agreement with the result obtained using the approximate Markov partitioning (which ensures the validity of the latter approximation). The above equation also exactly establishes the linear scaling relation of the mean lifetime about $\epsilon = 0$, with $\langle n \rangle$ diverging at $a_0 = 2$. By symmetry of the map, identical results will be obtained if we consider the trajectory switching from L to R.

Another interesting quantity which also shows a scaling behavior around $\epsilon = 0$, is the drift rate v from one subinterval to the other [14]. This measures the rate at which the chaotic trajectory switches between L and R. Owing to the symmetry $F(-x) = -F(x)$ of the DAT map, the net drift rate is zero, i.e., switching to either subinterval occurs equally often. Let us consider switching from R to L (identical results will hold for switching in the opposite direction due to symmetry). The drift rate is measured by the fraction of R mapping to L per iteration. Hence $v = \epsilon/(2+\epsilon)$. It is again a linear scaling relation as $a_0 \rightarrow 2$ from above. Note that, for $a_0 < 2$, $v = 0$ as the two subintervals are isolated from each other. Thus v is analogous to an order parameter, having a finite (positive) value above $a_0 = 2$ and zero below it. This suggests that the merging of the chaotic attractors at $a_0 = 2$ is akin to a critical phenomena, with the local slope a_0 as the tuning parameter.

A similar study was also conducted with additive perturbation for the above map. In this case the dynamical system is defined as follows: $x_{n+1} = F(x_n) + \delta \sin(2\pi\omega n)$. For $a = 1.9$ (say), the map has two disconnected subintervals, $L:[-1,0)$ and $R:(0,1]$. However, an additive perturbation of magnitude $\delta > 0.1$ causes a portion of L to diffuse into R in the positive half-cycle of the sinusoidal signal (of frequency ω). Similarly, in the negative half-cycle, a portion of the R interval diffuses into L. The long-term behavior of the map is described by a ''smeared-out'' DAT map with a width δ, rather than the ''crisp'' piecewise linear DAT map with $a_0 = 1.9$. This happens as the map performs a periodic vertical motion, causing a smearing out over time. The simulation results showed a nonmonotonic behavior for the response as either ω or a_0 was varied, keeping the other constant, but this was less marked than in the case of multiplicative perturbation. This work can be seen in context with studies conducted on the dynamics of the logistic map under parametric perturbation [15].

Low-dimensional discrete-time dynamical systems are amenable to several analytical techniques, and hence can be well understood compared to other systems. The examination of resonance phenomena in this scenario was for ease of numerical and theoretical analysis. However, it is reasonable to assume that similar behavior occurs in a higher-dimensional chaotic system described by both maps and differential equations.

The close resemblance of the merging of attractors with critical phenomena has possible relevance to SR in Ising systems. Although numerical studies have reported SR in a kinetic Ising system, it seems to be inconclusive as the primary peak strength of the normalized residence-time distribution shows only a monotonic behavior [16]. This response profile is identical to that observed in the DAT map for $a_0 < 2$. A study of kinetic aspects like hysteresis is planned, which should give information concerning the phase dependence of the resonance behavior.

The observation of SR in chaotic systems also has implications for the area of noisy information processing. It has been proposed that the sensory apparatus of several creatures use SR to enhance their sensitivity to weak external stimulus, e.g., the approach of a predator. Some experimental work on crayfish has provided supporting evidence for this assertion [17]. The above study indicates that external noise is not necessary for such amplification, as chaos in neural networks can enhance weak signals. As chaotic behavior is extremely common in a recurrent network of excitatory and inhibitory neurons, such a scenario is not entirely unlikely to have occurred in the biological world. This can, however, be confirmed only by further biological studies and detailed modeling of the phenomena.

[1] R. Benzi, A. Sutera, and A. Vulpiani, J. Phys. A **14**, L453 (1981).

[2] B. McNamara and K. Wiesenfeld, Phys. Rev. A **39**, 4854 (1989).

[3] G. Nicolis, C. Nicolis, and D. McKernan, J. Stat. Phys. **70**, 125 (1993).

[4] V. S. Anishchenko, A. B. Neiman, and M. A. Safanova, J. Stat. Phys. **70**, 183 (1993).

[5] A. Crisanti, M. Falcioni, G. Paladin, and A. Vulpiani, J. Phys. A **27**, L597 (1994).

[6] E. Reibold, W. Just, J. Becker, and H. Benner, Phys. Rev. Lett. **78**, 3101 (1997).

[7] L. Gammaitoni, F. Marchesoni, and S. Santucci, Phys. Rev. Lett. **74**, 1052 (1995).

[8] E. Ippen, J. Lindner, and W. L. Ditto, J. Stat. Phys. **70**, 437 (1993).

[9] T. L. Carroll and L. M. Pecora, Phys. Rev. Lett. **70**, 576 (1993).

[10] R. M. May, Ann. (N.Y.) Acad. Sci. **316**, 517 (1979); J. Testa and G. Held, Phys. Rev. A **28**, 3085 (1983).

[11] P. M. Gade, R. Rai, and H. Singh, Phys. Rev. E **56**, 2518 (1997).

[12] C. Seko and K. Takatsuka, Phys. Rev. E **54**, 956 (1996).

[13] R. M. Everson, Phys. Lett. A **122**, 471 (1987).

[14] S. Grossman and H. Fujisaka, Phys. Rev. A **26**, 1779 (1982).

[15] P. P. Saratchandran, V. M. Nandakumaran, and G. Ambika, Pramana, J. Phys. **47**, 339 (1996).

[16] S. W. Sides, R. A. Ramos, P. A. Rikvold, and M. A. Novotny, J. Appl. Phys. **81**, 5597 (1997); Phys. Rev. E (to be published) (http://xxx.lanl.gov/abs/cond-mat/9712021).

[17] J. K. Douglass, L. Wilkens, E. Pantazelou, and F. Moss, Nature (London) **365**, 337 (1993).